Expanded View Figures

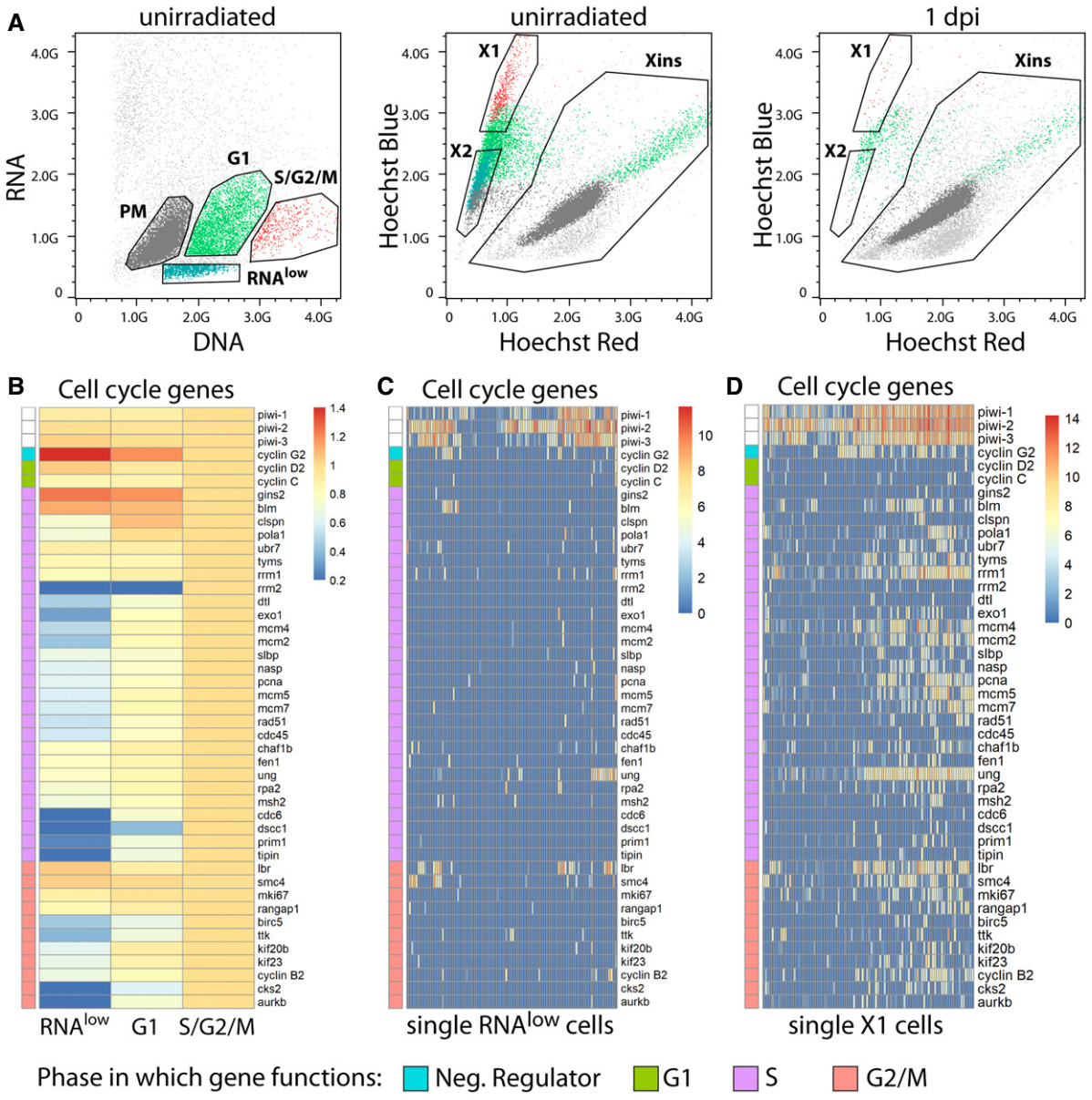

Figure EV1. Backgating and RNA-sequencing of DNA/RNA FACS gates.

A Backgating of the RNA^{low}, G1, S/G2/M, and PM populations from Hoechst/pyronin Y stained cells (left) onto a classic Hoechst side population plot (middle, unirradiated; right, 1 day post 60 Gy irradiation). Plots are representative of $n > 3$ independent experiments.

B Expression of cell cycle genes in bulk RNAseq data of RNA^{low}, G1 and S/G2/M cells. Heatmap scale, fold change of $\log_2$ normalized expression compared to S/G2/M.

C, D Expression of cell cycle genes in scRNAseq of 96 RNA^{low} neoblasts (C) or 96 previously sequenced X1 neoblasts (D, data ref: Molinaro & Pearson, 2016). Heatmap scale, log2 normalized expression level.

Data information: In (B–D), the cell cycle phase in which each gene primarily functions is indicated by the colour bar along the left side of each heatmap.

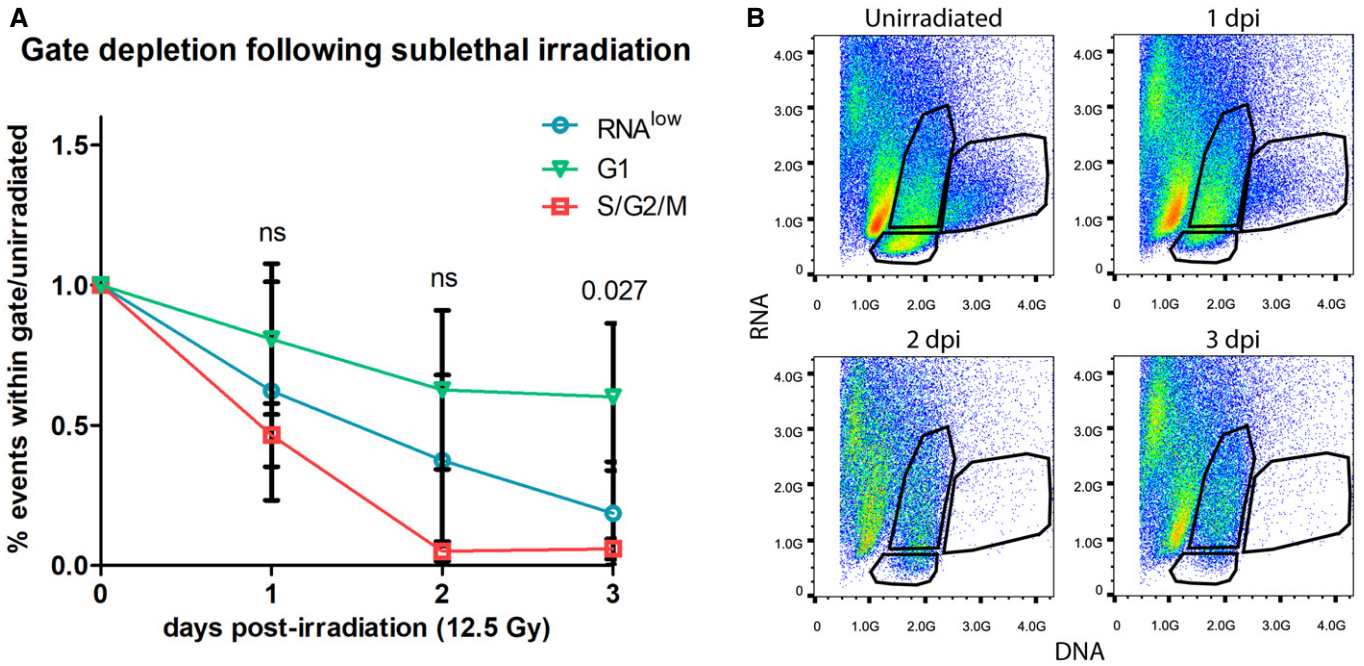

Figure EV2. Gate depletion kinetics following sublethal irradiation.

A Quantification of the proportion of events within the RNA^{low}, G1 or S/G2/M FACS gates in unirradiated controls and at 1–3 dpi (12.5 Gy of irradiation, $n = 3$ biological replicates). Data are normalized to unirradiated controls and presented as mean ± s.d. A one-way ANOVA was conducted to compare the depletion of each gate at a given time point. Gate depletion was not significant at 1 dpi ($F(2,6) = 1.12$, $P = 0.38$) or 2 dpi ($F(2,6) = 4.31$, $P = 0.069$). Gate depletion was significant at 3 dpi ($F(2,6) = 6.94$, $P = 0.027$). A post-hoc Turkey HSD test identified a significant difference between the G1 and S/G2/M gates at 3 dpi ($P = 0.027$).

B Representative FACS plots of the time course in (A). Plots are representative of $n = 3$ independent experiments.

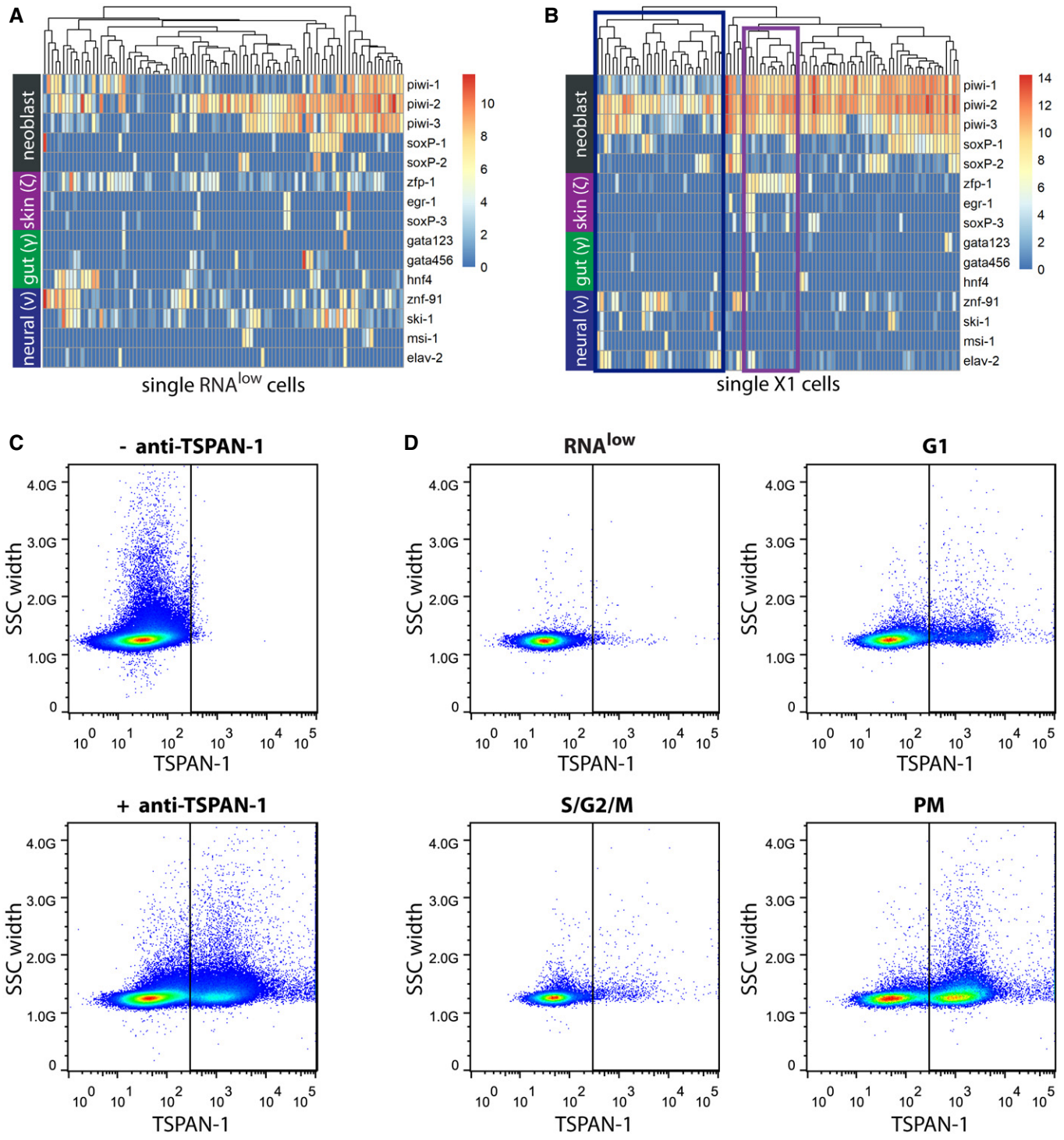

Figure EV3. The RNA^{low} gate likely contains a mix of lineage-committed and pluripotent neoblasts.

A, B Expression levels of general and lineage-committed neoblast markers in scRNAseq data of cells from the RNA^{low} gate (A) or previously sequenced X1 neoblasts (B, data ref: Molinaro & Pearson, 2016).Heatmap scale, log2 normalized expression level. Blue box, putative neural progenitor cluster; purple box, putative epithelial progenitor cluster.

C FACS plots showing TSPAN-1 immunostaining of whole dissociated animals without (top) or with (bottom) anti-TSPAN-1 antibody.

D FACS plots showing TSPAN-1 immunostaining of cells from the RNA^{low}, G1, S/G2/M, or PM gates.

Data information: In (C and D), plots are representative of $n = 4$ independent experiments. SSC, side scatter.

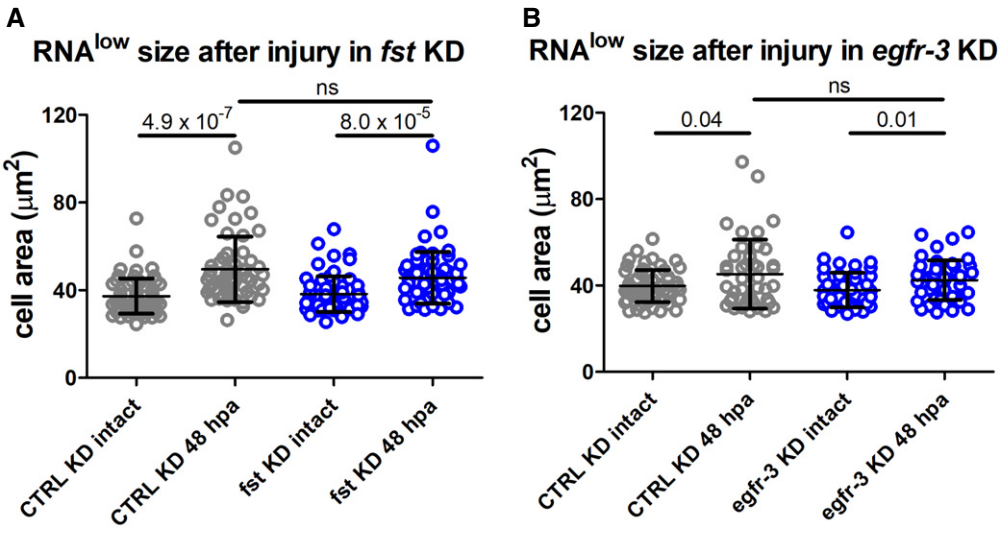

Figure EV4. *fst* and *egfr-3* are not required for the RNA^{low} neoblast growth response to injury.

A RNA^{low} neoblast size in intact animals and at 48-hpa in control or *fst* KD animals ($n \geq 56$).

B RNA^{low} neoblast size in intact animals and at 48-hpa in control or *egfr-3* KD animals ($n \geq 43$).

Data information: Data presented as mean ± s.d. Statistical significance was assessed using Welch's *t*-tests (*P* values are indicated; ns, not significant [$P > 0.05$]). In (A), animals were amputated at 4fd3. In (B), animals were amputated at 8fd3. The data are representative of 3 (A) or 2 (B) independent experiments.

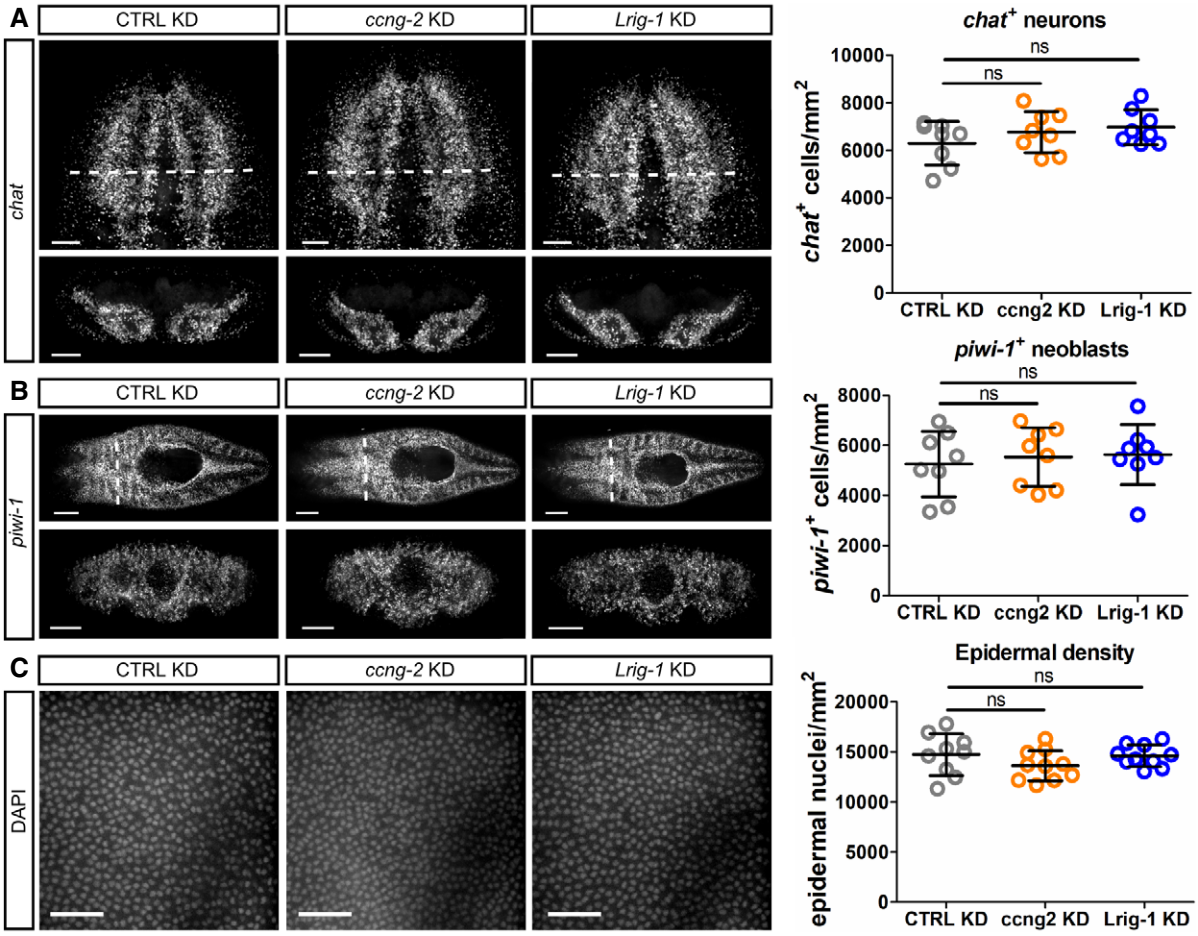

Figure EV5. No effect of *Lrig-1* knockdown on differentiation at homeostasis.

A–C Representative confocal images and quantifications of *chat*$^+$ neurons (A), *piwi-1*$^+$ neoblasts (B) and cell nuclei in the epidermis marked by DAPI (C) following control, *ccng2*, or *Lrig-1* knockdown at homeostasis (n = 8 technical replicates for all). Scale bars, 100 μm in (A); 250 μm in (B) (top panels) and 100 μm in (B) (bottom panels); 50 μm in (C).

Data information: Data presented as mean ± s.d. Statistical significance was assessed using Welch's t-tests (ns, not significant [$P > 0.05$]). Animals were fixed at 5fd5. In (A and B), images are maximum projections and bottom panels are cross-sections taken from the region indicated by the dashed white lines in the corresponding top panel. In (C), images are single confocal planes at the level of the epidermis. The data are representative of one independent experiment.